

# Bragg spectroscopy of trapped one dimensional strongly interacting bosons in optical lattices: Probing the cake-structure

Guido Pupillo<sup>1</sup>, Ana Maria Rey<sup>2</sup> and Ghassan George Batrouni<sup>3</sup>

<sup>1</sup>*Institute for Quantum Optics and Quantum Information of the Austrian Academy of Sciences, 6020 Innsbruck, Austria*

<sup>2</sup>*Institute for Theoretical Atomic, Molecular and Optical Physics,*

*Harvard-Smithsonian Center of Astrophysics, Cambridge, MA, 02138, USA and*

<sup>3</sup>*Institut Non-Linéaire de Nice, Université de Nice-Sophia Antipolis, 1361 Route des Lucioles, 06560 Valbonne, France*

(Dated: May 3, 2021)

We study Bragg spectroscopy of strongly interacting one dimensional bosons loaded in an optical lattice plus an additional parabolic potential. We calculate the dynamic structure factor by using Monte Carlo simulations for the Bose-Hubbard Hamiltonian, exact diagonalizations and the results of a recently introduced effective fermionization (EF) model. We find that, due to the system's inhomogeneity, the excitation spectrum exhibits a multi-branched structure, whose origin is related to the presence of superfluid regions with different densities in the atomic distribution. We thus suggest that Bragg spectroscopy in the linear regime can be used as an experimental tool to unveil the shell structure of alternating Mott insulator and superfluid phases characteristic of trapped bosons.

## I. INTRODUCTION

Cold atoms in optical lattices provide a way for realizing interacting many body systems in essentially defect free lattices [1]. Paradigms of strongly correlated phenomena such as the superfluid (SF) to Mott insulator (MI) quantum phase transition have been realized in a three-dimensional lattice thanks to the successful application of atom optics techniques to traditional condensed matter systems [2]. Recently, much interest has been generated by experiments in reduced dimensionality [3, 4, 5, 6, 7, 8], where the role of interactions and quantum fluctuations is enhanced. Of particular relevance have been the realization of a SF/MI quantum phase transition in one-dimension (1D) [4, 8], and the observation of a gas of hard core bosons [3, 4, 5], or Tonks-Girardeau (TG) gas [9]. The latter is a characteristic of strongly interacting one dimensional systems, where the large repulsion between atoms mimics the Pauli exclusion principle. As a consequence, there is a one to one correspondence of the eigenenergies and eigenfunctions of TG bosons and non-interacting fermions. This correspondence holds for all local observables, such as the atomic density and fluctuations [9].

The presence in experiments of a confining parabolic potential superimposed on the lattice provides the possibility of studying strongly correlated systems at arbitrary densities. In fact, the presence of the quadratic potential typically induces the coexistence of alternating superfluid and insulating phases with on-site lattice densities which can be larger than one [1, 10, 11, 12]. This creates a shell structure, which is reminiscent of the MI lobes of the homogeneous phase diagram [13]. In this case, the SF/MI transition is better understood as a crossover than as a phase transition [11]. Recently, it was shown that a system of strongly interacting 1D bosons at high densities has the structure of an array of stacked disjoint TG gases [14]. This decomposition of the system in independent TG gases, or *effective fermionization* (EF), allows for the computation of static properties such as the density profile and fluctuations, as well as dynamical properties. In particular, EF has been used to explain the microscopic mechanisms respon-

sible for the decay of the superfluid current of an interacting bosonic gas in a periodic potential [7].

It remains a challenge to engineer experimental probes for atoms in the strongly correlated regime. Information on the excitation spectrum has been obtained by using Bragg spectroscopy [8], sparking considerable theoretical activity [15, 16, 17, 18]. Unfortunately, the experiment of Ref. [8] was conducted in a regime far from linear, which prevented the direct comparison of the theoretical results with the experimental data. In particular, in the case of the inhomogeneous system it has not been possible to verify the nature of the double peak structure found in Ref. [17] in the low frequency response, by direct comparison to the existing data of Ref. [8].

In this paper we study Bragg spectroscopy of bosons in the periodic plus quadratic potentials in the linear response regime. We perform quantum Monte Carlo simulations and exact diagonalizations of the Bose-Hubbard Hamiltonian in the strongly interacting regime to compute the dynamic structure factor. The latter is found to exhibit a multi-branched structure at small excitation frequencies [17]. We compare these numerical results to the predictions of the EF model, finding good agreement. The central result of this paper is that this agreement strongly indicates that this multi-branched structure at low-frequency is dominated by the excitations of the system's superfluid components. That is, the observed different excitation branches can be attributed primarily to the response of the superfluid components of the various layers of the EF model, whose presence is directly linked to the existence of a shell structure in the many body density profile. When there are at least two superfluid regions with different mean particle numbers, as is the case of Ref. [8], this result differs substantially from previous results, where the presence of the double-peak structure in the response to the Bragg perturbation was linked to the presence of particle-hole excitations in the Mott phase [17]. Therefore, because of the sensitivity to the presence of superfluids with different particle numbers, we suggest that Bragg spectroscopy in the linear regime is an ideal tool to characterize the shell structure of atoms in the quadratic potential (see also [19, 20, 21]).

The presentation of the results is organized as follows. In Sec. II we introduce the Bose-Hubbard Hamiltonian, shortly review the physics of strongly interacting bosons in a lattice and explain the basic ideas of the effective fermionization model. In Sec. III we introduce the dynamic structure factor. In Sec. IV we compare the results of the EF model and of exact diagonalizations for a small number of bosons in a homogenous lattice. The various branches of excitation are explained in terms of (low-frequency) excitations of the superfluid and (higher-frequency) particle-hole excitations. The EF model is shown to well reproduce the excitations of the superfluid. In Sec. V we compare the results of quantum Monte-Carlo simulations for experimentally realistic systems to the results of the EF model. When there are more than one superfluid regions with different particle densities, we show strong evidence that the low-frequency excitations are dominated by the excitations of the various superfluids. We then propose an experiment in the linear response regime which would detect the associated shell structure of the many-body density profile. Finally, the conclusions are presented in Sec. VI.

## II. BOSE-HUBBARD HAMILTONIAN

The Bose-Hubbard (BH) Hamiltonian describes  $N$  interacting bosons in a lattice potential of  $M$  sites [1]

$$\hat{H} = \sum_j \left[ \Omega j^2 \hat{n}_j + \frac{U}{2} \hat{n}_j (\hat{n}_j - 1) - J (\hat{a}_j^\dagger \hat{a}_{j+1} + \hat{a}_{j+1}^\dagger \hat{a}_j) \right]. \quad (1)$$

Here  $\hat{a}_j$  is the bosonic annihilation operator at site  $j$ , and  $\hat{n}_j = \hat{a}_j^\dagger \hat{a}_j$ .  $\Omega$  is the curvature of the confining potential and  $U$  and  $J$  are the on-site interaction and hopping energies.

In the homogeneous system,  $\Omega = 0$ , the effective strength of the interactions depends on the atomic density  $N/M$ , and the ratio  $\gamma = U/J$ . In particular, for  $N < M$  the system is effectively a strongly interacting TG gas if  $U$  is larger than the lattice band width  $4J$  [4]. Thus,  $\gamma = \gamma_c \approx 4$  determines the critical interaction strength in low density systems. In particular, the SF/MI transition occurs in a homogeneous unit filled lattice at  $\gamma \approx \gamma_c$ . For arbitrarily large densities,  $n - 1 < N/M \leq n$ , with  $n$  an integer larger than one, the system enters the strongly correlated regime when  $\gamma \gg \gamma_c n$ . In these cases standard fermionization techniques are invalid, however the low energy physics can still be well reproduced by considering the excess  $M[N - (n - 1)]$  bosons as non-interacting fermions with an effective kinetic energy  $nJ$  sitting on a plateau formed by  $M(n - 1)$  atoms frozen in a Mott state with exactly  $n - 1$  atoms per site. The validity of this approximation relies on the fact that states with more than  $n$  atoms per site are suppressed by a factor on the order of  $1/\gamma$ . In other words, when  $\gamma \gg \gamma_c n$ , the whole many-body system can be conveniently visualized as composed of two independent subsystems: the atoms frozen in the Mott state and the extra TG bosons [14].

For most experiments, a parabolic magnetic confining potential of frequency proportional to  $\Omega$  is also present, so the density profile varies across the lattice. In the trapped case the

conditions for the formation of a Mott state change dramatically. For example, it is always possible to create a unit-filled MI if  $N < M$ , by varying the depth of the lattice or the magnetic trap frequency. In the trivial  $J = 0$  limit, the density profile becomes a “cake” structure with maximal occupation  $n^*$  at the trap center. In our model, we view the density as a “layer cake” of  $n$  stacked horizontal layers. When  $J = 0$ , the atoms are completely frozen, and each layer of the cake may be viewed as an independent Mott state with  $N_n$  unit-filled sites.

For moderate values of  $J > 0$ , it has been shown theoretically that the density profile still has a cake structure of coexisting superfluid and MI phases. In this case, the density profile can be visualized as being composed of stacked horizontal layers, but because atoms are no longer frozen, in general the layers are not independent. However, if number fluctuations in adjacent horizontal layers do not overlap in space, all layers can be treated independently and, as in the homogeneous system, standard fermionization techniques can be applied to each layer separately. In this situation single-particle solutions provide expressions for all many-body observables. We call this generalization of the Bose-Fermi mapping *extended fermionization* (EF).

We want to point out that at variance with the original definition [14], and for the sake of simplicity, we here refer to all kinds of strongly interacting gases as EF, independently of the density and the presence or absence of an external potential. In the low density limit  $n = 1$ , EF reduces to standard fermionization.

In the remainder of this paper we focus on this strongly correlated regime, where  $\gamma \gg \gamma_c n$ . Because  $J$  decreases exponentially with increasing lattice depth, this regime is easily attained experimentally.

## III. THE DYNAMIC STRUCTURE FACTOR

The dynamic structure factor at temperature  $T$  is given by:

$$S(q, \omega) = \frac{1}{\mathcal{Z}} \sum_{ji} e^{-\beta E_i} |\langle i | \hat{\rho}_q | j \rangle|^2 \delta(\hbar\omega - E_i + E_j), \quad (2)$$

where,  $\mathcal{Z}$  is the canonical partition function,  $\beta^{-1} = T k_B$ , with  $k_B$  the Boltzmann constant and  $T$  the temperature. Here,  $E_j$  are the eigenenergies of the many body eigenstates  $|i\rangle$ , and  $\hat{\rho}_q = \frac{1}{M} \sum_j e^{iqdj} \hat{a}_j^\dagger \hat{a}_j$  is the density fluctuation operator with  $\hbar q$  the quasi-momentum and  $d$  the lattice constant. For the quantum Monte Carlo simulations we use a World-line algorithm at small finite temperature  $T k_B = 0.1 J$  [17, 22], while for the exact diagonalizations we use standard linear algebra techniques, and  $T$  can be taken to be zero. Equation (2) describes the response of the system to Bragg spectroscopy in the linear response regime. It implies that the system responds whenever the frequency  $\omega$  of the Bragg perturbation matches the energy difference between two eigenstates.

For  $\gamma \gg \gamma_c n$  and at low enough energy, eigenstates are densely grouped in energy ranges of the order of a few  $J$  [24], separated by an energy of the order of  $U$ . Eigenstates in each

energy range are linear combinations of Fock states with the same number of empty sites, of singly occupied sites, doubly occupied sites, and so on. We thus expect that in the strongly correlated regime the system's response to the Bragg perturbation mirrors the "grouped" structure of the many body energy spectrum.

In standard fermionization,  $S(q, \omega)$  is obtained by computing Eq. (2) for a system of non-interacting fermions [23].

$$S(q, \omega) = \sum_{nm} \left| \sum_j e^{-iqdj} \psi_j^{(n)} \psi_j^{(m)} \right|^2 f(E^{(n)}) [1 - f(E^{(m)})] \times \delta(\hbar\omega - E^{(n)} + E^{(m)}). \quad (3)$$

Here  $\psi_j^{(n)}$  and  $E^{(n)}$  are the  $n^{\text{th}}$  single-particle eigenmodes and eigenenergies of Eq.(1) with hopping energies  $J$  respectively and  $j$  is the lattice site index.  $f(E^{(n)})$  denotes the Fermi-Dirac distribution.

For the cases when there are more than one atom per site, according to the EF model the density profile can be visualized as being composed of stacked horizontal layers. In the parameter regime where number fluctuations in adjacent horizontal layers do not overlap in space, all layers can be treated independently and the dynamical structure factor of the overall system can be approximated by adding the structure factors of the  $n$  different layers each one with  $N_n$  atoms. The expression for  $S(q, \omega)$  in a given  $n$  layer is exactly the same than Eq.(3) but replacing the eigenmodes and eigenenergies by the single-particle solutions of Eq.(1) with hopping energies  $nJ$ . Also the chemical potential in the Fermi-Dirac distributions must be calculated to consistently have an average of  $N_n$  atoms in each layer.

The independent addition of the structure factor of each layer is justified in the model, because EF takes into account only the responses of the superfluids to the Bragg perturbation. Thus, when the two superfluid regions are spatially well separated, matrix elements coupling low-lying excitations of the two superfluids in Eq. (2) become zero, because of the vanishing overlap of the wave functions.

#### IV. HOMOGENEOUS LATTICE ( $\Omega = 0$ )

In Fig. 1 we show  $S(q, \omega)$  as a function of the Bragg frequency  $\omega$ , for a homogeneous lattice with  $M = 6$  and periodic boundary conditions. The number of atoms is  $N = 5$  (panels (a) and (c)) and  $N = 7$  (panels (b) and (d)). The temperature  $T$  is equal to zero, in all the plots. The continuous, dashed and dotted lines correspond to different quasi-momenta, with  $qd = \pi/3, 2\pi/3$  and  $\pi$ , respectively. Panels (a) and (b) are the results of exact diagonalizations with  $\gamma = 10$ , while panels (c) and (d) are the predictions of the EF model for atoms with kinetic energy  $J$  and  $2J$ , respectively. In Fig.1(a) the exact results show large peaks for  $\hbar\omega/J \lesssim 4$ , and smaller excitations for  $8 \lesssim \hbar\omega/J \lesssim 14$ . The value  $4J$  corresponds to the single particle band width of a hole, that is of an empty site tunneling in the lattice. These low frequency excitations are thus due to the coupling between the ground state and eigenstates with

at most one atom per site. The smaller peaks in the interval  $8 \lesssim \hbar\omega/J \lesssim 14$  are instead due to the coupling to particle-hole excitations (1-ph), that is to eigenstates which have one site occupied by two atoms and an extra empty site. Accordingly, these peaks are centered around the value  $\hbar\omega = U$ . The reduced intensity of the 1-ph peaks with respect to the lowest energy peaks is expected, since in first-order perturbation theory the coupling of the ground state to 1-ph is proportional to  $1/\gamma$ . In fact as analytically calculated in Ref. [16], for a unit filled system the height of the particle hole peaks is proportional to  $64/\gamma^2$  which is of the order observed in the plot. Panel (c) shows that the position and the height of the lowest energy peaks are reasonably well reproduced by the EF model, since  $n = 1$ . This is remarkable, since  $\gamma$  is only 10 in Fig.1(a), while it is considered infinite in the model. On the other hand, the high energy peaks are missing, since 1-ph are not present in the model [14].

The qualitative analysis above is easily adapted to the case  $M = 6, N = 7$  of panels (b) and (d). Here,  $n = 2$  and the EF model predicts that the low energy spectrum is the one of a single particle with hopping energy  $2J$  on top of a plateau of 6 atoms, which are frozen in a unit-filled Mott insulator. Thus,  $S(q, \omega)$  in the EF model reduces to computing Eq. (2) for a non-interacting fermion with hopping energy  $2J$ . Since the single particle band width is now  $8J$ , we expect a large low frequency response in the energy range  $\hbar\omega/J \leq 8$ . This is actually shown in Figs. 1(b) and (d), which confirms the validity of the EF model even for such a small value of  $\gamma$ . In fact, the latter is just barely larger than  $2\gamma_c = 8$ . In addition, the exact results of Fig. 1(b) show excitations around  $\hbar\omega \approx U$ . Not surprisingly, the latter are due to coupling to eigenstates with two sites occupied by two atoms, and to eigenstates with

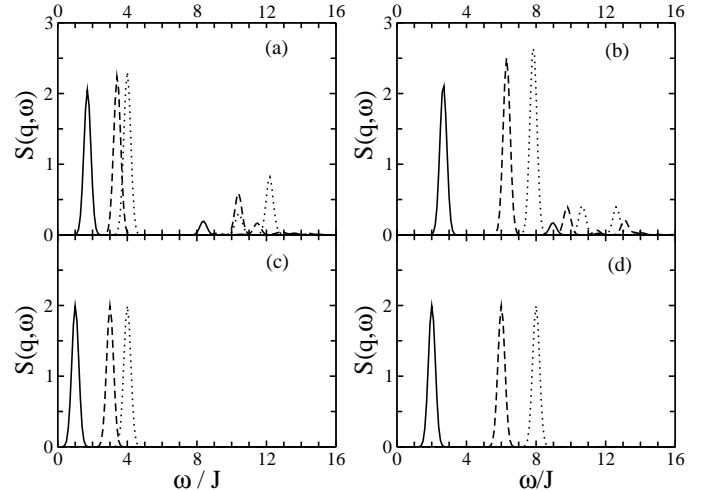


FIG. 1: The dynamic structure factor  $S(q, \omega)$  vs  $\omega$ , with  $qd = \pi/3$  (continuous line),  $2\pi/3$  (dashed line) and  $\pi$  (dotted line). Here,  $M = 6$  in all panels, while  $N = 5$  (panels (a) and (c)) and  $N = 7$  (panels (b) and (d)). Panels (a) and (b) are results of exact diagonalizations with  $\gamma = U/J = 10$ , while panels (c) and (d) are the EF model results. For all plots,  $\Omega/J = 0$ .

a site occupied by three atoms. These couplings are again proportional to  $1/\gamma$ , and thus the height of these high energy peaks is highly suppressed. We have also found numerically excitations at an energy of order  $2U$ . Because the couplings of these eigenstates to the ground state are of order  $1/\gamma^2$ , these peaks are very small, and are not shown in the graphs.

Finally, we checked numerically that in the case  $M = N = 6$ , where the ground state is a Mott insulator with one atom per site, the lowest energy peaks are centered around  $U$ . The spectrum is thus gapped, in this case, as expected. The peaks' height is of the same order of magnitude of the peaks of Figs. 1(a) and (b) centered around  $\hbar\omega \approx U$ . A comprehensive discussion of the excitations in the MI phase can be found in Ref. [16]. In the following we show how the above discussion is useful in the description of the spectrum of excitations when the quadratic trap is present.

### V. INHOMOGENEOUS LATTICE ( $\Omega > 0$ )

When the quadratic trap is present and  $\gamma > \gamma_c$ , the system can show the coexistence of superfluid and insulating phases. Figure 2 displays the local density profiles of systems with such coexisting SF and MI phases, with onsite peak density one, (a), and larger than one, (b). In the plots, integer and non-integer local densities signal MI and SF phases, respectively. Here,  $M = 100$  and  $\Omega = 0.008J$ . In Fig. 2(a) the value of  $\gamma$  is 14, while it is  $\gamma = 8$  in Fig. 2(b). These values and the fillings we use are comparable to those used in current experiments. The continuous (red) and dashed (black) lines are the quantum Monte Carlo data and the predictions of the EF model, respectively. The two curves are almost indistinguishable on the scale of the graph, which is remarkable at least for the results of panel (b), where the EF model at the center of the trap is barely applicable. For the case of Fig. 2(a) where the peak on-site density is one, the EF model corresponds to standard fermionization. On the other hand, for the case of Fig. 2(b), the EF model amounts to decomposing the density profile into two vertically stacked horizontal layers of atoms [14] (with  $N_1 = 61$  and  $N_2 = 3$  atoms in the lower and upper layers, respectively). In Fig. 2(b) atoms in the lowest layer have been shaded, in order to visualize the two layers of the EF model. In each layer there is at most one atom per site, and thus the EF idea is to apply standard fermionization techniques to each layer separately. Then, it is possible to calculate many body observables (e.g., the density profile) for the two layers separately, and add the results to obtain the total value. Details of the computation for the density profile are given in Ref. [14]. There, it is shown that EF provides accurate results whenever the superfluid regions at the trap center and at the edges are spatially well separated by sufficiently large MI regions. In fact, in this case it is possible to unambiguously attribute a certain number of atoms to each layer of the EF model, so that layers are well defined. This is the case of Fig. 2(b), where an insulating region of about 10 lattice sites separates the superfluids at the trap center and at the edges. In the following we compute  $S(q, \omega)$  for the two layers separately and then add the obtained results to calculate the complete  $S(q, \omega)$ .

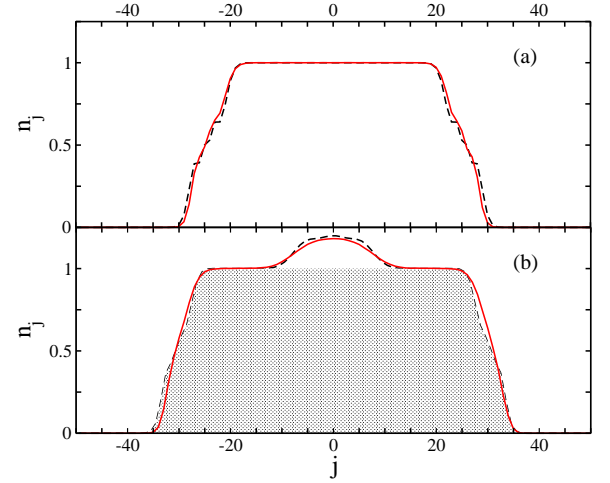


FIG. 2: (Color online) Local density profile,  $n_j$ , as a function of the lattice site  $j$  for the confined system with  $M = 100$ , and  $\Omega/J = 0.008$ . Panel (a):  $N = 50$  and  $\gamma = 14$ . Panel (b):  $N = 64$  and  $\gamma = 8$ . The continuous (red) and dashed (black) lines are the quantum Monte Carlo and EF model results, respectively. The shaded area in panel (b) corresponds to atoms in the lowest layer of the EF model. These atoms are largely frozen in a unit-filled Mott's state, analogous to the case of panel (a).

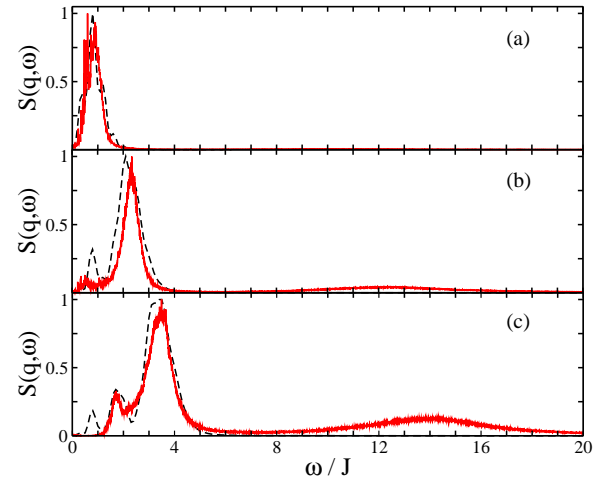


FIG. 3: (Color online)  $S(q, \omega)$  vs  $\omega$  for the system in Fig. 2(a) with  $N = 50$ ,  $\gamma = 14$ , and for  $qd = 0.2\pi$ (a),  $0.5\pi$ (b), and  $0.9\pi$ (c). The continuous (red) and dashed (black) lines are the quantum Monte Carlo and EF model results, respectively. The large excitation peaks for  $\hbar\omega/J < 4$  are excitations of the superfluid component, while the broad peak at  $\hbar\omega \approx U = 14J$  is due to particle-hole excitations of the combined SF and MI, analogous to Fig. 1.

Figure 3 shows  $S(q, \omega)$  as a function of  $\omega$  for some values of  $q$  for the system of Fig. 2(a), where there is at most one atom per site. In particular, Figs. 3(a), (b) and (c) correspond to  $qd = 0.2\pi$ ,  $0.5\pi$  and  $0.9\pi$ , respectively. In the calculations we have normalized the height of the largest peak to 1. Analogous to the case of Fig. 1(a), the numerical solution shows



large peaks in the energy range  $\hbar\omega \leq 4J$ . The EF solution, which here reduces to standard fermionization, captures the location and width of these peaks rather well. Since fermionization accounts only for couplings to states with at most one atom per site, we conclude that the response for  $\hbar\omega/J \leq 4$  is solely due to the small number of atoms in sites  $|j| \geq 20$  which are in the superfluid phase (analogous to the discussion of Fig. 1(a)). These are thus “surface” excitations. In addition, for  $q$  large enough ( $qd \sim \pi$ ) the numerical solution shows the presence of peaks around  $U$ , which are not captured by the EF model. These are due to couplings to 1-ph excitations, in analogy to the discussion above. Therefore, the excitation spectrum exhibits two branches, a lower energy one corresponding to excitations of the surface superfluid layer and a higher one corresponding to the Mott region.

The differences between the numerical and EF results can be attributed both to errors of order  $\sim 1/\gamma^2$  in the EF predictions and to the fact that the numerical calculation of  $S(q, \omega)$  is difficult for  $\gamma \gg 1$ . In this respect, we notice that the lowest energy excitation in the EF model is always at  $\hbar\omega \approx \Omega N = 0.4J$ , which is the energy cost for an atom at position  $N/2$  (farthest outlying occupied site), to tunnel to the next unoccupied site. The fact that the numerical results do not grab this excitation for  $qd \sim \pi$  (Fig. 3(c)) suggests a partial failure of the numerics.

Similarly, Fig. 4 shows  $S(q, \omega)$  (normalized to 1) as a function of  $\omega$  at different values of  $q$  for the case of Fig. 2(b), where there is a superfluid phase at the trap center with more than one atom per site. The continuous (red) line is the Monte Carlo result, while the dashed (black) line is the EF model result. As mentioned above, the EF model assumes that the system of Fig. 2(b) is conveniently decomposed into two disjoint, vertically stacked gases, each one with at most one atom per site. Most atoms in the lowest layer are frozen in a Mott insulator state, in analogy to the case of Fig 3(a), while atoms in the upper layer are delocalized in a region approximately comprising the sites  $-10 \leq j \leq 10$ . Atoms in the lower and upper layers have hopping energies  $J$  and  $2J$ , respectively, and are treated as independent. The results for  $S(q, \omega)$  for the lower and upper layers are indicated by dotted lines (green and blue lines respectively).

Figure 4 shows that the numerical excitation spectrum (continuous line) at large enough momenta has two branches of excitations, which saturate at  $\hbar\omega \approx 4J$  and  $8J$ , respectively. The existence of these two branches of excitation has been previously reported by one of us in Ref. [17], where the lower and higher frequency peaks were attributed to excitations of the SF and MI phases respectively, as in the case of Fig. 3. However, while this interpretation is correct for Fig. 3, it is only partially so in this case. The good agreement between the numerical results and the results of the EF model (dashed line) with respect to the position and width of the large feature around  $\hbar\omega \approx 4J$ , and the position of the peak around  $\hbar\omega \approx 8J$  for large  $q$ , strongly suggests that this double peak structure is mainly due to excitations of the superfluid components of the two layers of the EF model. In particular, the lower frequency excitations ( $\hbar\omega \leq 4J$ ) are due to superfluid atoms in the lowest layer of the EF model (sites where  $n_j < 1$ ,

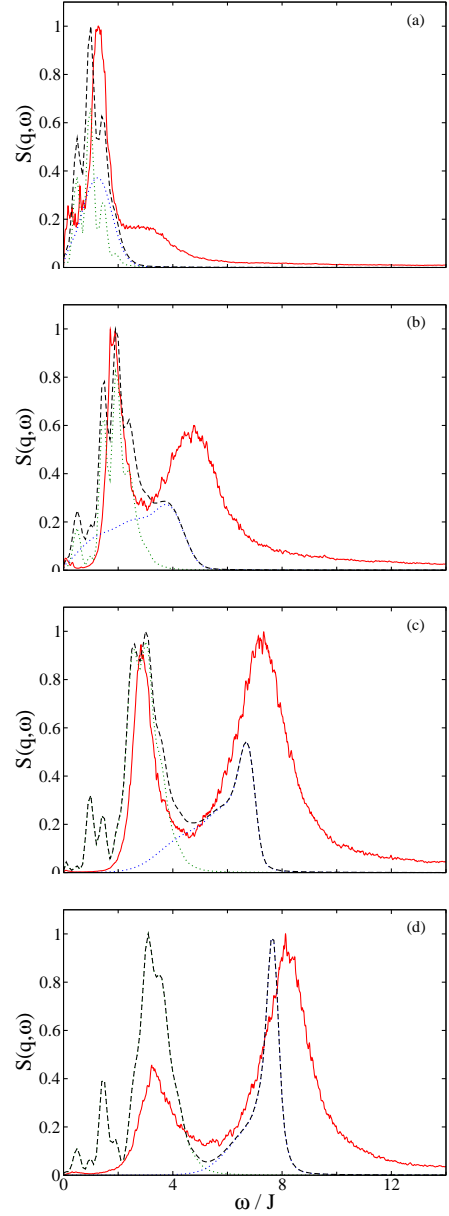


FIG. 4: (Color online)  $S(q, \omega)$  vs  $\omega$  for the system in Fig. 2(b) with  $N = 64$ ,  $\gamma = 8$ , and for  $qd = 0.2\pi$ (a),  $0.4\pi$ (b),  $0.7\pi$ (c), and  $0.9\pi$ (d). The continuous (red) and dashed (black) lines are the quantum Monte Carlo and EF model results, respectively. The dotted lines are results for the lower (green) and upper (blue) layers of the EF model. The dashed line is thus obtained by adding these curves. The excitation peak saturating at  $\hbar\omega/J \approx 4$  is due to excitations in the SF with less than one atom per site, ( $n_j < 1$ , with  $25 \leq |j| \leq 35$  in Fig. 2(b)). The excitation peak saturating at  $\hbar\omega/J \approx 8$  is due to excitations in the SF with more than one atom per site, ( $n_j > 1$ , with  $0 \leq |j| \leq 10$  in Fig. 2(b)). Because  $\gamma = 8$ , particle-hole excitations around  $\hbar\omega/J \approx 8$  increase the width of this SF peak in the Monte Carlo results.

in the shaded region of Fig. 2), while the higher frequency excitations are mostly due to excitations of atoms in the upper layer, which are all in the SF phase. As mentioned above, the saturation thresholds  $4J$  and  $8J$  correspond to the values of the effective single particle band-widths of atoms with hopping energy  $J$  and  $2J$ , respectively.

Since here  $\gamma = 8$ , 1-ph excitations certainly do contribute to the system's response around  $\hbar\omega/J = 8$ . However, since the coupling to 1-ph excitations in the linear regime is rather suppressed, as can be seen in Fig. 3 (it is proportional to  $1/\gamma$ ), we argue that the intensity of the response peak centered around  $\hbar\omega \approx 8J$  is dominated by the excitations of SF atoms in the second layer rather than by 1-ph excitations. Unfortunately, a detailed discussion of Fig. 4 is complicated by the fact that the discrepancies between the model and Monte-Carlo results are most likely of physical as well as computational nature. As said above, the physical origin of the discrepancies resides in the EF model neglecting 1-ph excitations. This contributes to the underestimation of the height and width of the peak around  $\hbar\omega \approx 8J$  in the EF results of Fig. 4(c) (while the peak around  $\hbar\omega \approx 4J$  is well reproduced). On the other hand, because the relative height of the peaks in the numerical solution varies greatly from  $qd = 0.7\pi$  (panel (c)) to  $qd = 0.9\pi$  (panel (d)) and oscillates in between (not shown), we are also led to suppose the existence of some instability in the numerical results. This prevents us from attributing unambiguously all the discrepancies between the numerical and model results to 1-ph excitations, and thus getting a quantitative estimate of 1-ph contributions to the excitation spectrum.

With all the *provisos* above, we can safely state that an important effect of coupling to 1-ph excitations is to increase the width of the peak around  $\hbar\omega \approx 8J$  with respect to the EF results. That is, by increasing the ratio  $\gamma$ , we would expect to see a continuous decrease of the width of the peak at  $\hbar\omega/J = 8$ , and the growth of a distinct peak at the chosen  $\gamma$ -value. This new distinct peak would be due to 1-ph excitations of the atoms in the two layers, analogous to the discussion of Fig. 1(a-b).

In other words, the presence of a multiply peaked structure in the low frequency response to the Bragg perturbation for  $\gamma \gg nJ$  is clear evidence of the existence of a shell structure in the many body density profile (Fig. 2). In fact, for  $qd \approx \pi$  the peak corresponding to the superfluid component of a generic layer  $n$  saturates at  $\hbar\omega \approx 4nJ$ , and thus the presence of low-frequency peaks separated by  $4J$  is an indication of the cloud's shell structure. We thus propose to use Bragg spectroscopy to characterize the various phases of the trapped strongly correlated bosons, by detecting this multiple peak structure. For example, the system's response could be measured in successive experiments while keeping fixed the trapping potentials (and thus the  $\gamma$  and  $\Omega/J$  ratios), and

varying the total number of atoms  $N$ . Then, for  $qd \approx \pi$  and  $N < \sqrt{4U/\Omega}$  a single peak at  $\omega \approx 4J$  would be observed ( $\sqrt{4U/\Omega}$  is a threshold value for having only one layer in the EF model, [14]). By increasing  $N$  to values larger than  $\sqrt{4U/\Omega}$  a peak at  $\hbar\omega/J \approx 8$  would be suddenly observed in the system's response, signaling the formation of a SF with two atoms per site at the trap center. By further increasing  $N$ , other peaks would occur at multiples of  $4J$ , signaling the formation of superfluid regions with more than two atoms per site. It should be noted that typically the lifetime of these states would be severely limited by three-body recombination, and the observation of these layers may become complicated.

Finally, we notice that Bragg spectroscopy in the linear regime may also be used to detect the atoms' shell structure in dimensions  $D$  larger than one (where fermionization techniques are not applicable). In fact, in the appropriate parameter regimes, the system retains the structure of an array of vertically stacked horizontal layers. Thus, the response to the Bragg perturbation of atoms in the superfluid regions of the different layers should provide for a signature of the shell structure. Since the kinetic energy is a factor of  $D$  larger, the various branches of excitations at low frequency should be more separated for  $D > 1$  than for  $D = 1$ . This may facilitate the experimental resolution of the excitation peaks in dimensions higher than one.

## VI. SUMMARY

We have presented a study of the dynamical structure factor for strongly interacting bosons confined in homogeneous lattices and in presence of a quadratic confining potential. By comparing the results of quantum Monte Carlo simulations and exact diagonalizations with the predictions of an analytical EF model, we characterized the excitation spectrum of strongly correlated bosons at arbitrary densities. In particular, we were able to identify low frequency peaks in the system's response to the Bragg perturbation which are clear cut evidence of the formation of a shell structure in the density profile. This shell structure is made of alternating SF and MI phases, which we propose to study using Bragg spectroscopy in the linear response regime.

We thank R. T. Scalettar, F. F. Assaad and M. Köhl for very helpful discussions. G.P. acknowledges support from the EU through a grant of the OLAQUI Project. A.M.R. acknowledges support from a grant of the Institute of Theoretical, Atomic, Molecular and Optical Physics at Harvard University and Smithsonian Astrophysical observatory.

- 
- [1] D. Jaksch *et al.*, Phys. Rev. Lett. **81**, 3108 (1998).
  - [2] M. Greiner *et al.*, Nature **415**, 39 (2002).
  - [3] B. Laburthe Tolra *et al.*, Phys. Rev. Lett. **92**, 190401 (2004).
  - [4] B. Paredes *et al.*, Nature **429**, 277 (2004).

- [5] T. Kinoshita *et al.*, Science **305**, 1125 (2004).
- [6] H. Moritz *et al.*, Phys. Rev. Lett. **91**, 250402 (2003).
- [7] C.D. Fertig *et al.*, Phys. Rev. Lett. **94**, 120403 (2005).
- [8] T. Stöferle *et al.*, Phys. Rev. Lett. **92**, 130403 (2004).

- [9] M. Girardeau, J. Math. Phys. **1**, 516 (1960).
- [10] V.A. Kashurnikov *et al.*, Phys. Rev. A **66**, 031601(R) (2002).
- [11] G.G. Batrouni *et al.*, Phys. Rev. Lett. **89**, 117203 (2002).
- [12] B. DeMarco *et al.*, Phys. Rev. A **71**, 063601 (2005).
- [13] M.P.A. Fisher *et al.*, Phys. Rev. B **40**, 546 (1989).
- [14] G. Pupillo *et al.*, cond-mat/0505325 (2005).
- [15] D. Van Oosten *et al.*, Phys. Rev. A **71**, 021601(R) (2005).
- [16] A.M. Rey *et al.*, Phys. Rev. A **72**, 023407 (2005).
- [17] G.G. Batrouni *et al.*, Phys. Rev. A **72**, 031601(R) (2005).
- [18] A. Iucci *et al.*, cond-mat/0508054 (2005).
- [19] F. Gerbier *et al.*, Phys. Rev. Lett. **95**, 050404 (2005).
- [20] F. Gerbier *et al.*, Phys. Rev. A **72**, 053606 (2005).
- [21] P. Sengupta *et al.*, Phys. Rev. Lett. **95**, 220402 (2005).
- [22] G.G. Batrouni and R. Scalettar, Phys. Rev. B **46**, 9051 (1992).
- [23] P. Vignolo and A. Minguzzi, J. Phys. B: At. Mol. Opt. Phys. **34**, 4653 (2001).
- [24] G. Pupillo *et al.*, Phys. Rev. A **68**, 063604 (2003).